

## Recognition of bio-relevant dicarboxylate anions by an azacalix[2]arene[2]triazine derivative decorated with urea moieties

Miguel Santos,<sup>a,b</sup> Igor Marques,<sup>a</sup> Sílvia Carvalho,<sup>a</sup> Cristina Moiteiro<sup>\*b</sup> and Vítor Félix<sup>\*a</sup>

<sup>a</sup> Departamento de Química, CICECO and iBiMED, Universidade de Aveiro, 3810-193 Aveiro, Portugal.

<sup>b</sup> Centro de Química e Bioquímica, DQB, Faculdade de Ciências, Universidade de Lisboa, Campo Grande, 1749-016 Lisboa, Portugal.

### Contents

Contents .....	1
Figures index .....	2
Tables index .....	3
<sup>1</sup> H and <sup>13</sup> C NMR spectra .....	4
Mass spectra .....	9
Infrared spectra.....	12
VT <sup>1</sup> H NMR .....	15
X-ray Crystallography.....	16
NMR titrations.....	18
Job plots.....	22
Molecular dynamics .....	24

## Figures index

Figure S1. $^1\text{H}$ NMR spectrum of <b>3</b> in $\text{CDCl}_3$ .....	4
Figure S2. $^{13}\text{C}$ APT NMR spectrum of <b>3</b> in $\text{CDCl}_3$ .....	4
Figure S3. $^1\text{H}$ NMR spectrum of <b>4</b> in $\text{CDCl}_3$ .....	5
Figure S4. $^{13}\text{C}$ APT NMR spectrum of <b>4</b> in $\text{CDCl}_3$ .....	5
Figure S5. $^1\text{H}$ NMR spectrum of <b>5</b> in $\text{CD}_3\text{CN}$ .....	6
Figure S6. $^1\text{H}$ NMR spectrum of <b>6</b> in $\text{DMSO-d}_6$ .....	6
Figure S7. $^1\text{H}$ NMR spectrum of <b>7</b> in $\text{DMSO-d}_6$ .....	7
Figure S8. $^{13}\text{C}$ APT NMR spectrum of <b>7</b> in $\text{DMSO-d}_6$ .....	7
Figure S9. $^1\text{H}$ NMR spectrum of <b>1</b> in $\text{CDCl}_3$ .....	8
Figure S10. $^{13}\text{C}$ APT NMR spectrum of <b>1</b> in $\text{CDCl}_3$ .....	8
Figure S11. LRMS (ESI) spectrum of <b>3</b> .....	9
Figure S12. LRMS (ESI) spectrum of <b>4</b> .....	9
Figure S13. HRMS (ESI) spectrum of <b>7</b> .....	10
Figure S14. Isotopic distribution of $[\text{M}+\text{H}]^+$ ion in the HRMS (ESI) spectrum of <b>7</b> .....	10
Figure S15. HRMS (ESI) spectrum of <b>1</b> .....	11
Figure S16. Isotopic distribution of $[\text{M}+\text{H}]^+$ ion in the HRMS (ESI) spectrum of <b>1</b> .....	11
Figure S17. FTIR spectrum of <b>3</b> (KBr) .....	12
Figure S18. FTIR spectrum of <b>4</b> (KBr) .....	12
Figure S19. FTIR spectrum of <b>6</b> (KBr) .....	13
Figure S20. FTIR spectrum of <b>7</b> (KBr) .....	13
Figure S21. FTIR spectrum of <b>1</b> (KBr) .....	14
Figure S22. $^1\text{H}$ NMR spectra of <b>1</b> at 293, 269, 257, 245 and 234 K in $\text{CDCl}_3$ .....	15
Figure S23. Close-up of H-13 and H-16 signals in the $^1\text{H}$ NMR spectra of <b>1</b> at 293, 269, 257, 245 and 234 K in $\text{CDCl}_3$ .....	15
Figure S24. Atomic notation scheme of for the urea binding units of the four independent molecules (A-D) of <b>1</b> .....	16
Figure S25. Relevant sections of $^1\text{H}$ NMR spectra in $\text{CDCl}_3$ of free <b>1</b> and upon addition of 0.1, 0.9, 2.8 and 4.0 equivalents of $\text{ox}^{2-}$ .....	18
Figure S26. Relevant sections of $^1\text{H}$ NMR spectra in $\text{CDCl}_3$ of free <b>1</b> and upon addition of 0.1, 0.9, 2.8 and 4.0 equivalents of $\text{mal}^{2-}$ .....	18
Figure S27. Relevant sections of $^1\text{H}$ NMR spectra in $\text{CDCl}_3$ of free <b>1</b> and upon addition of 0.1, 0.9, 2.8 and 4.0 equivalents of $\text{suc}^{2-}$ .....	19
Figure S28. Relevant sections of $^1\text{H}$ NMR spectra in $\text{CDCl}_3$ of free <b>1</b> and upon addition of 0.1, 0.9, 2.8 and 4.0 equivalents of $\text{dg}^{2-}$ .....	19
Figure S29. Relevant sections of $^1\text{H}$ NMR spectra in $\text{CDCl}_3$ of free <b>1</b> and upon addition of 1.1 and 2.8 equivalents of ( <i>S,S</i> )- and ( <i>R,R</i> )-tart $^{2-}$ .....	20
Figure S30. Relevant sections of $^1\text{H}$ NMR spectra in $\text{CDCl}_3$ of free <b>1</b> and upon addition of 1.1 and 2.8 equivalents of fum $^{2-}$ and male $^{2-}$ .....	20
Figure S31. Job plot for <b>1</b> · $\text{ox}^{2-}$ in $\text{CDCl}_3$ .....	22
Figure S32. Job plot for <b>1</b> · $\text{mal}^{2-}$ in $\text{CDCl}_3$ .....	22
Figure S33. Job plot for <b>1</b> · $\text{suc}^{2-}$ in $\text{CDCl}_3$ .....	22
Figure S34. Job plot for <b>1</b> · $\text{glu}^{2-}$ in $\text{CDCl}_3$ .....	22
Figure S35. Job plot for <b>1</b> · $\text{dg}^{2-}$ in $\text{CDCl}_3$ .....	22
Figure S36. Job plot for <b>1</b> ·( <i>S,S</i> )-tart $^{2-}$ in $\text{CDCl}_3$ .....	22
Figure S37. Job plot for <b>1</b> ·( <i>R,R</i> )-tart $^{2-}$ in $\text{CDCl}_3$ .....	23
Figure S38. Job plot for <b>1</b> ·fum $^{2-}$ in $\text{CDCl}_3$ .....	23

Figure S39. Job plot for <b>1</b> ·male <sup>2-</sup> in CDCl <sub>3</sub> .....	23
Figure S40. 3-D histogram for the third MD run of <b>1</b> ·suc <sup>2-</sup> (left), and the respective type A (center) and type B (right) binding scenarios. Each carboxylate unit (shown either in red or blue) is represented by the positions occupied by its oxygen atoms, 5 or more times.....	25
Figure S41. MD simulation cell of the system with the suc <sup>2-</sup> anion complex, showing the position of the TBA counter-ions in the beginning (left) and at the end of the equilibration stage. The TBA molecules are shown in space-filling mode, with the carbon atoms in magenta.....	25
Figure S42. Electrostatic potential mapped on the molecular electron density surface (0.001 electrons per Bohr <sup>3</sup> ) of mal <sup>2-</sup> , suc <sup>2-</sup> , dg <sup>2-</sup> , fum <sup>2-</sup> and male <sup>2-</sup> . The $V_{S,\min}$ and $V_{S,\text{carb}}$ are respectively represented by blue and green dots on the molecular surfaces. The colour scales range from blue to red as follows: mal <sup>2-</sup> [-242.8; -158.5 kcal mol <sup>-1</sup> ]; suc <sup>2-</sup> [-207.7; -152.0 kcal mol <sup>-1</sup> ]; dg <sup>2-</sup> [-222.4; -135.2 kcal mol <sup>-1</sup> ]; fum <sup>2-</sup> [-206.7 ; -160.3 kcal mol <sup>-1</sup> ]; and male <sup>2-</sup> [-229.8 ; -132.9 kcal mol <sup>-1</sup> ]. .....	26
Figure S43. Sketch of tetraazacalix[2]arene[2]triazine derivatives showing the atom types' positions. The R <sub>1</sub> , R <sub>2</sub> and R <sub>3</sub> substituents are given in Table S8.....	27

## Tables index

Table S1. Dimensions of N-H···O hydrogen bonds of <b>1</b> .....	16
Table S2. Crystal data and structure refinement details for (NMe) <sub>4</sub> -azacalix[2]arene[2]triazine <b>1</b> .....	17
Table S3. Proton resonances used in the determination of $K_{ass}$ for the associations between <b>1</b> and the dicarboxylate anion series ox <sup>2-</sup> , mal <sup>2-</sup> , suc <sup>2-</sup> , glu <sup>2-</sup> and dg <sup>2-</sup> .....	21
Table S4. Proton resonances used in the determination of $K_{ass}$ for the associations between <b>1</b> and the dicarboxylate anions ( <i>S,S</i> )-, ( <i>R,R</i> )-tart <sup>2-</sup> , fum <sup>2-</sup> and male <sup>2-</sup> .....	21
Table S5. Receptor's N <sub>urea</sub> ···N <sub>urea</sub> distances for the associations between <b>1</b> and ox <sup>2-</sup> , mal <sup>2-</sup> , suc <sup>2-</sup> , glu <sup>2-</sup> , dg <sup>2-</sup> , fum <sup>2-</sup> and male <sup>2-</sup> .....	24
Table S6. Average ${}^1\text{O}_2\text{C}\cdots\text{CO}_2^-$ distances collected for the associations between <b>1</b> and ox <sup>2-</sup> , mal <sup>2-</sup> , suc <sup>2-</sup> , glu <sup>2-</sup> , dg <sup>2-</sup> , male <sup>2-</sup> and fum <sup>2-</sup> .....	25
Table S7. Additional force field parameters used to model the tetraazacalix[2]arene[2]triazine derivatives.....	26
Table S8. RMSD values (Å) between the single crystal structures of tetraazacalix[2]arene[2]triazine derivatives and gas-phase structures obtained MM energy minimization with GAFF default parameters (GFD) and optimized parameters (OPT), respectively.....	27

<sup>1</sup>H and <sup>13</sup>C NMR spectra

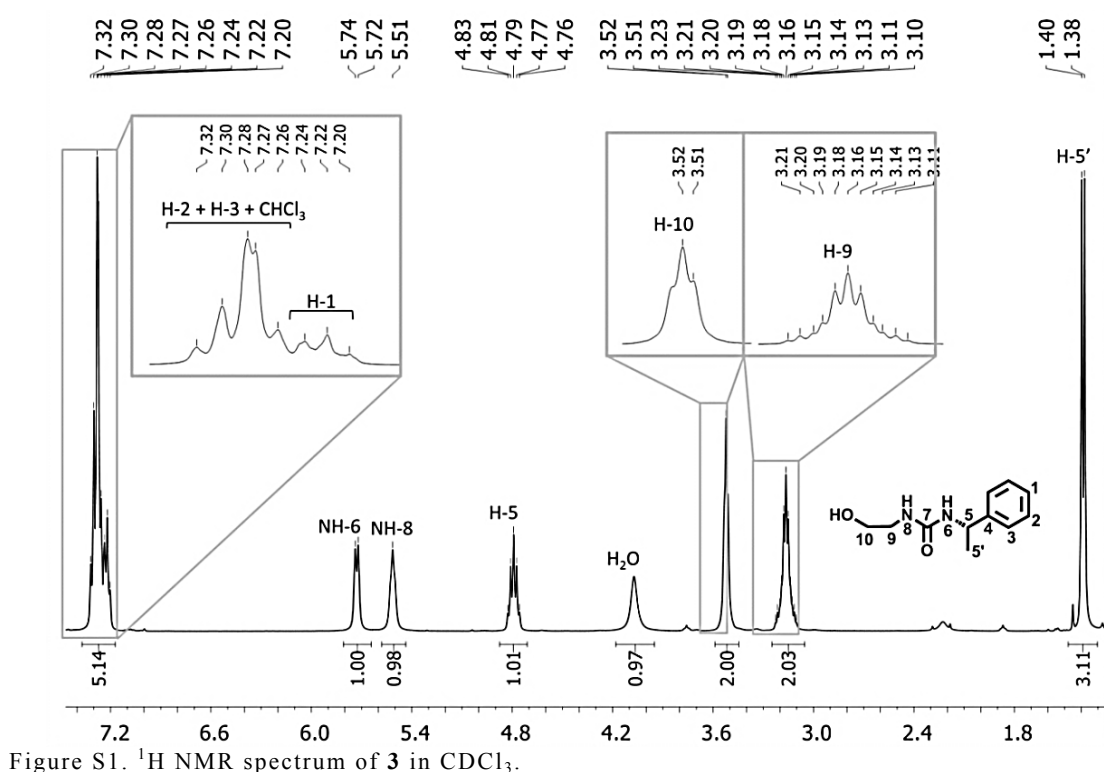


Figure S1. <sup>1</sup>H NMR spectrum of **3** in CDCl<sub>3</sub>.

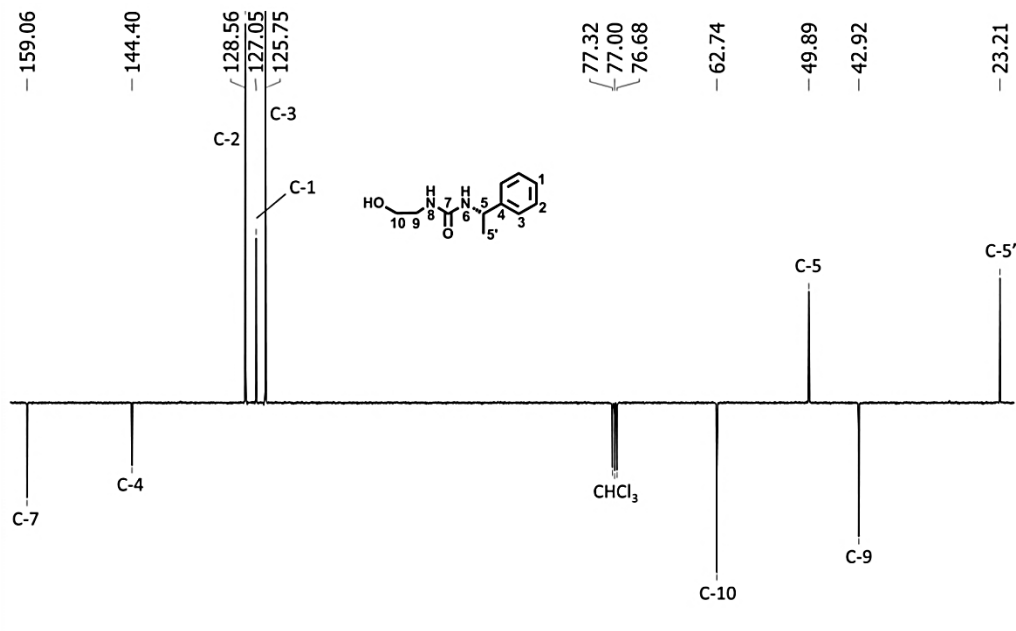


Figure S2. <sup>13</sup>C APT NMR spectrum of **3** in CDCl<sub>3</sub>.

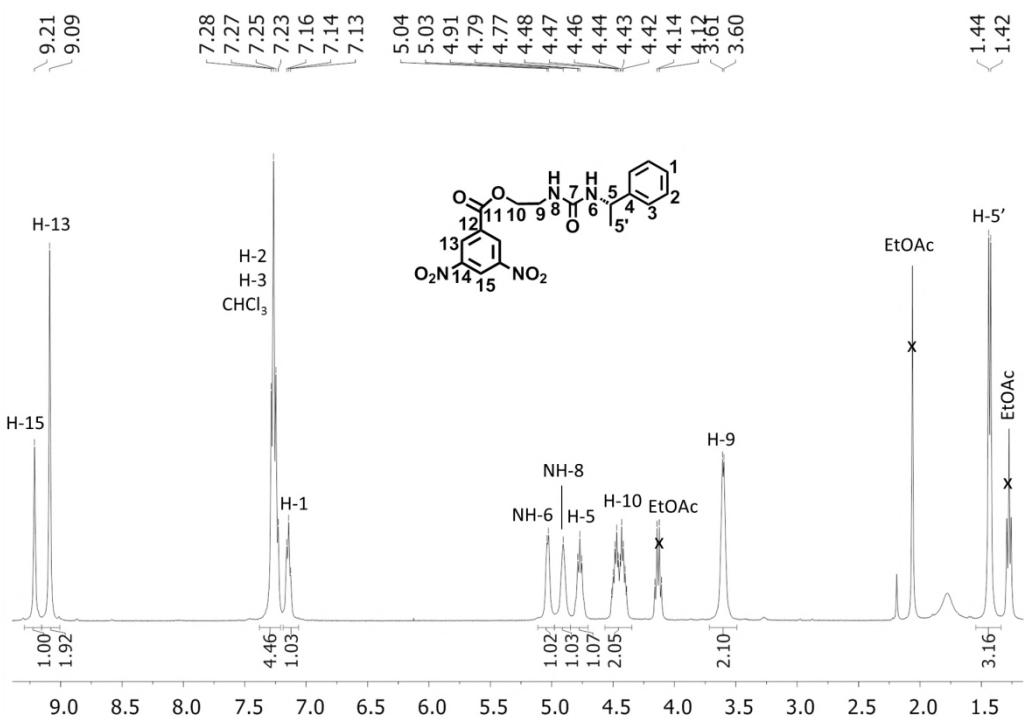


Figure S3.  $^1\text{H}$  NMR spectrum of **4** in  $\text{CDCl}_3$ .

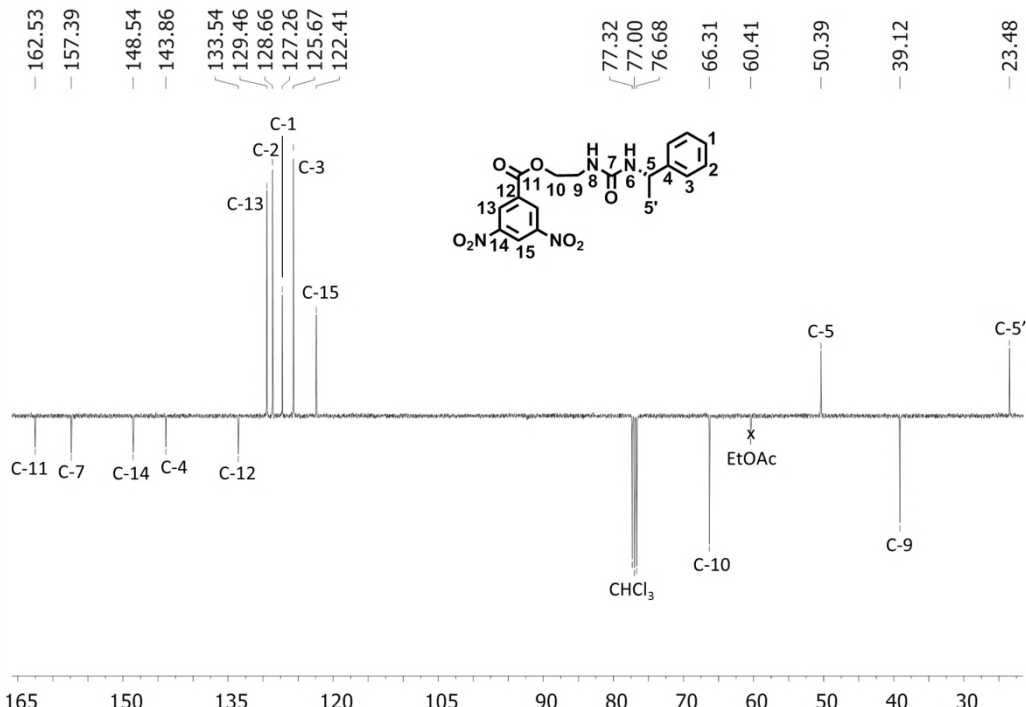


Figure S4.  $^{13}\text{C}$  APT spectrum of **4** in  $\text{CDCl}_3$ .

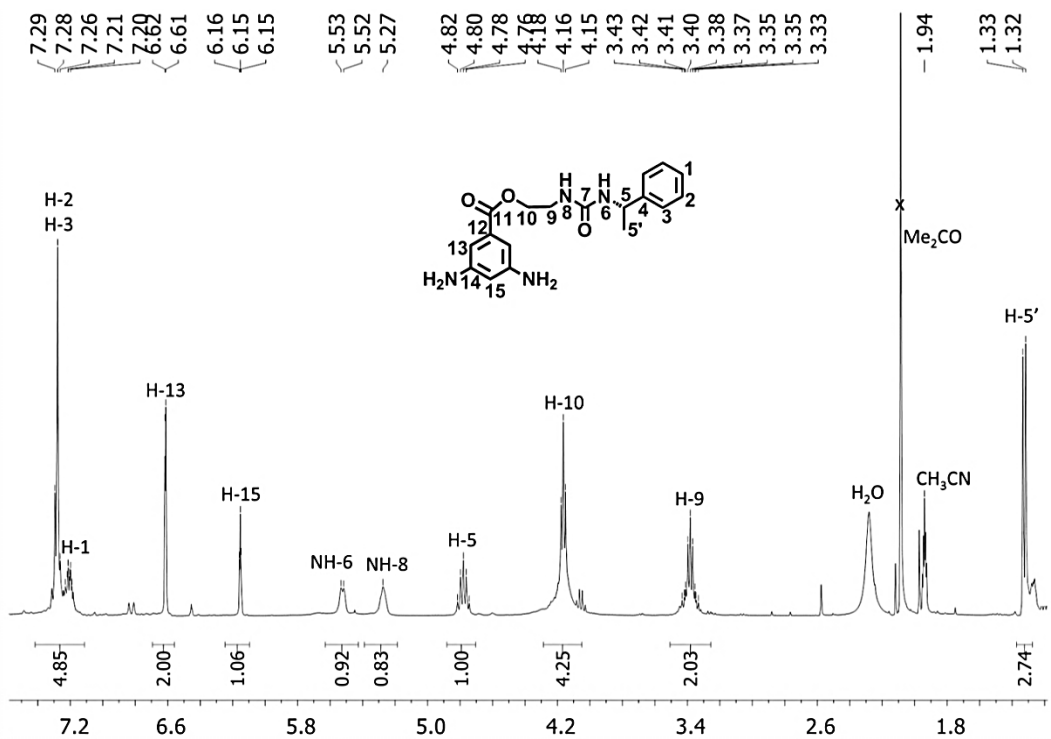


Figure S5. <sup>1</sup>H NMR spectrum of **5** in  $\text{CD}_3\text{CN}$ .

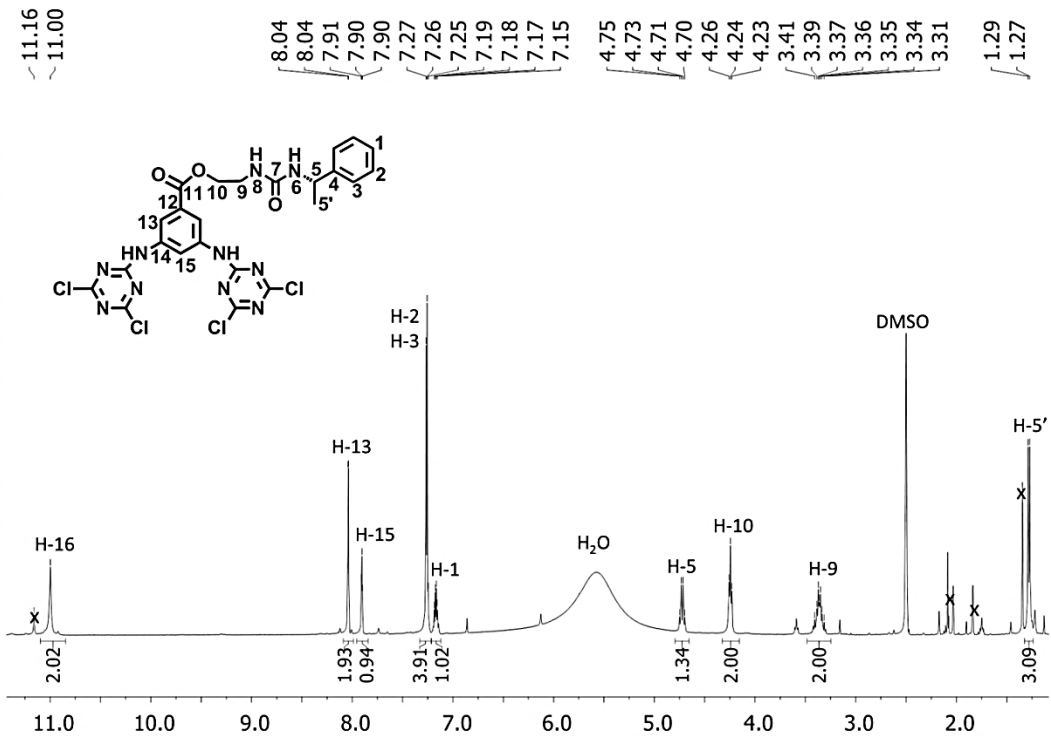


Figure S6. <sup>1</sup>H NMR spectrum of **6** in  $\text{DMSO-d}_6$ .

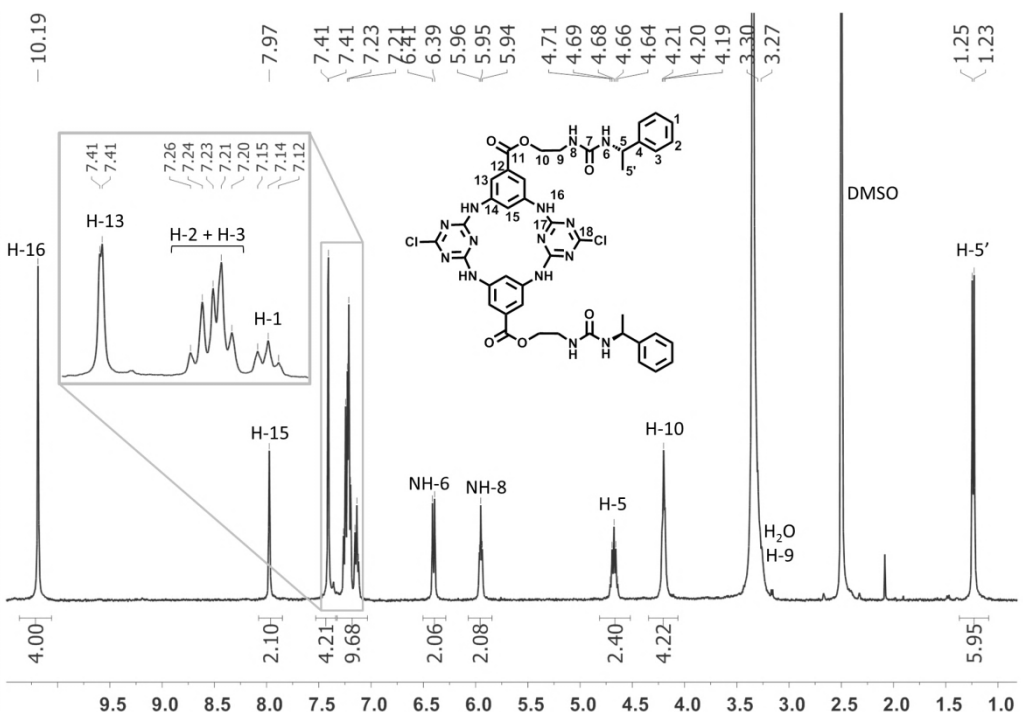


Figure S7.  $^1\text{H}$  NMR spectrum of **7** in  $\text{DMSO-d}_6$ .

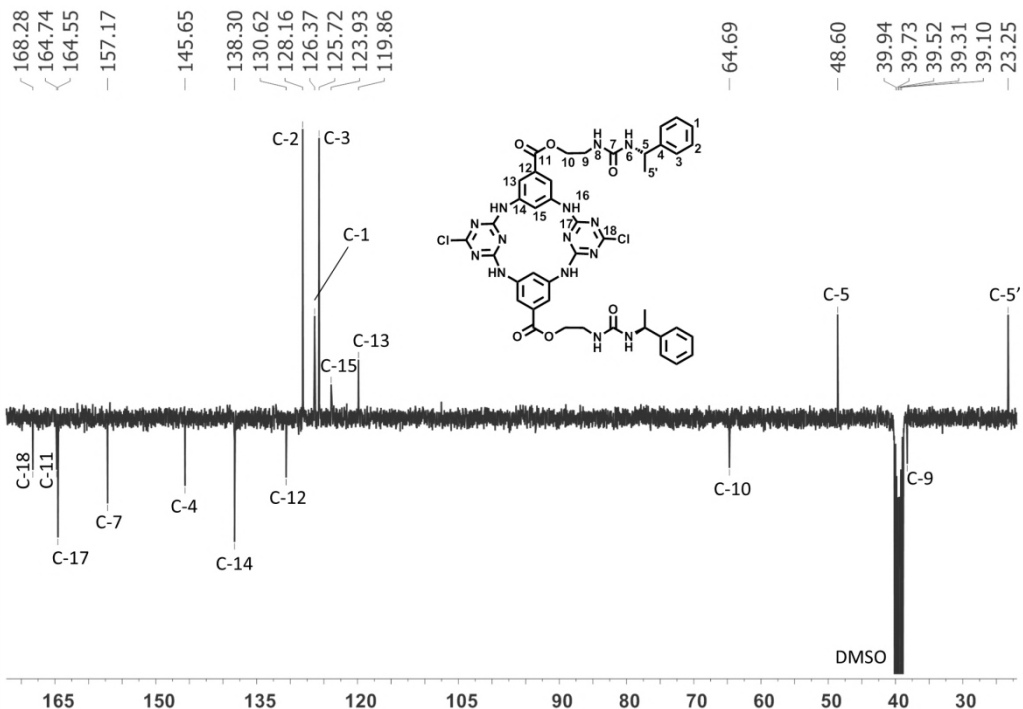


Figure S8.  $^{13}\text{C}$  APT NMR spectrum of **7** in  $\text{DMSO-d}_6$ .

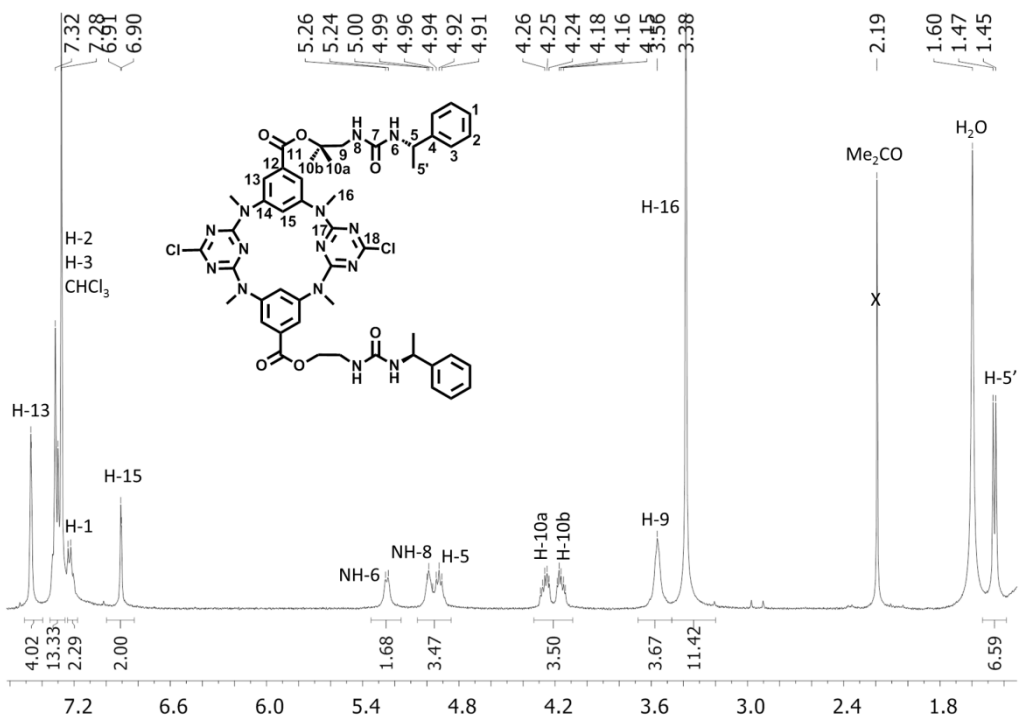


Figure S9.  $^1\text{H}$  NMR spectrum of **1** in  $\text{CDCl}_3$ .

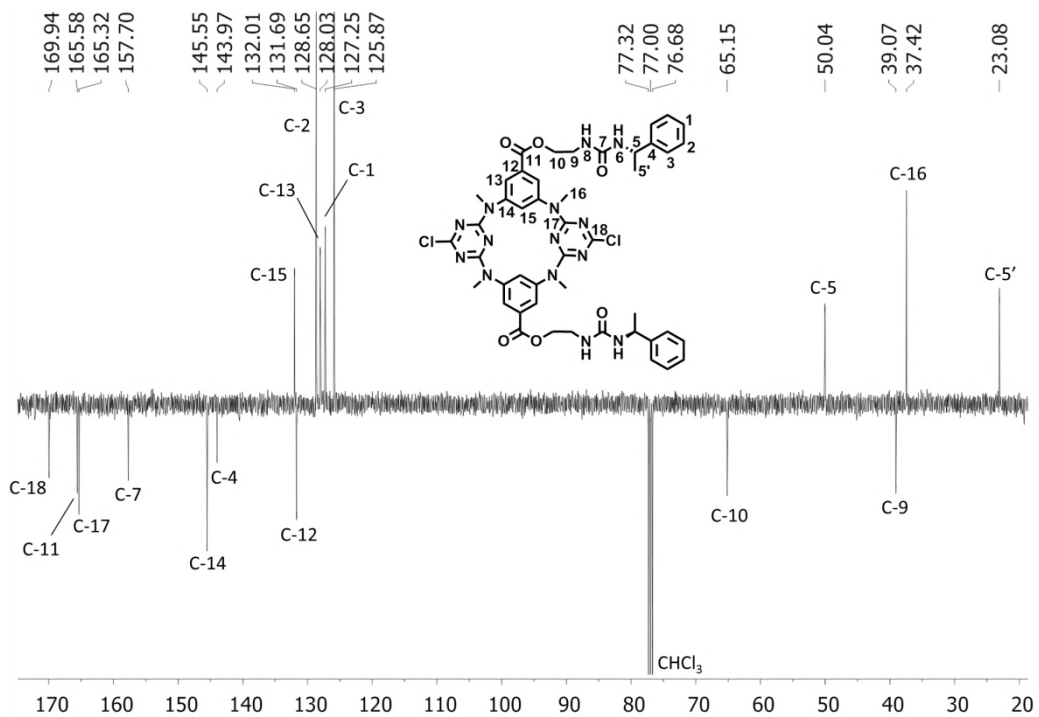


Figure S10.  $^{13}\text{C}$  APT NMR spectrum of **1** in  $\text{CDCl}_3$ .

## Mass spectra

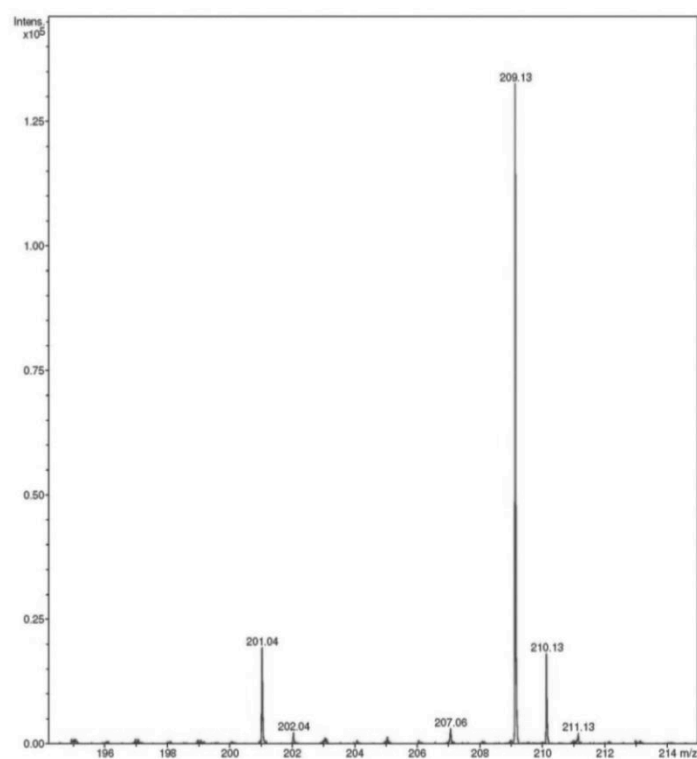


Figure S11. LRMS (ESI) spectrum of **3**.

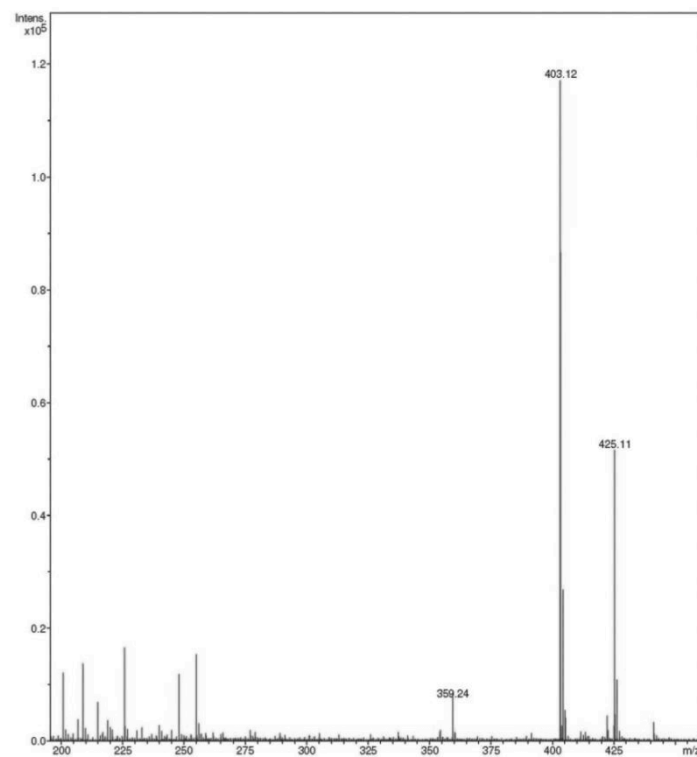


Figure S12. LRMS (ESI) spectrum of **4**.

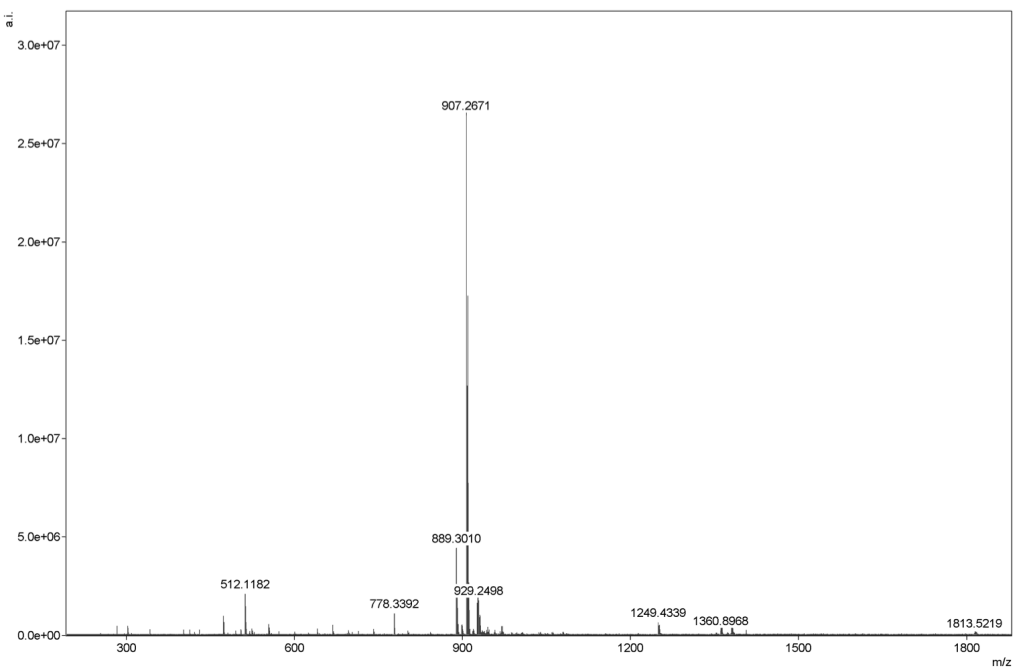


Figure S13. HRMS (ESI) spectrum of 7.

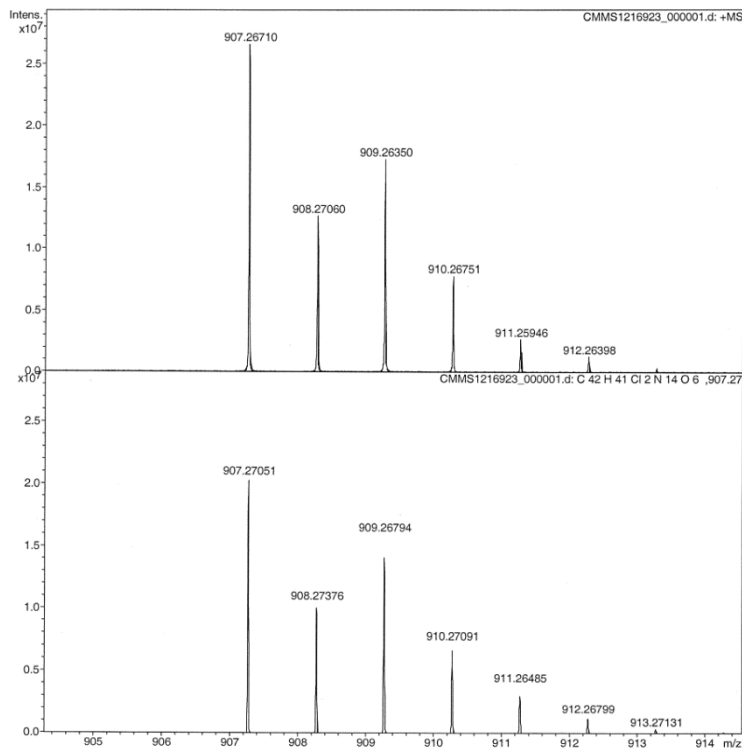


Figure S14. Isotopic distribution of  $[M+H]^+$  ion in the HRMS (ESI) spectrum of 7.

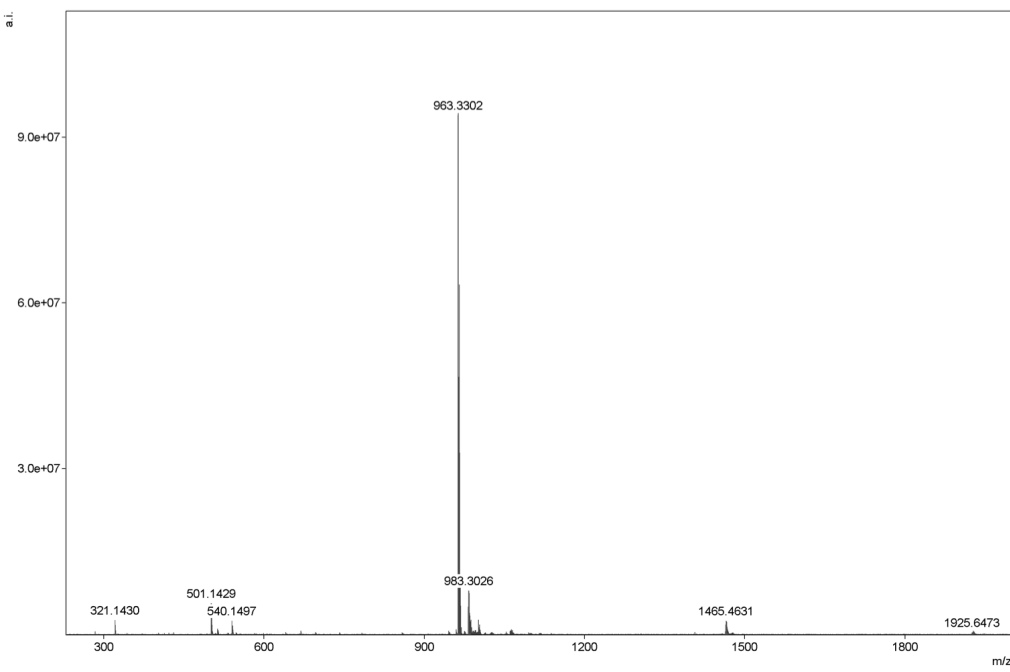


Figure S15. HRMS (ESI) spectrum of **1**.

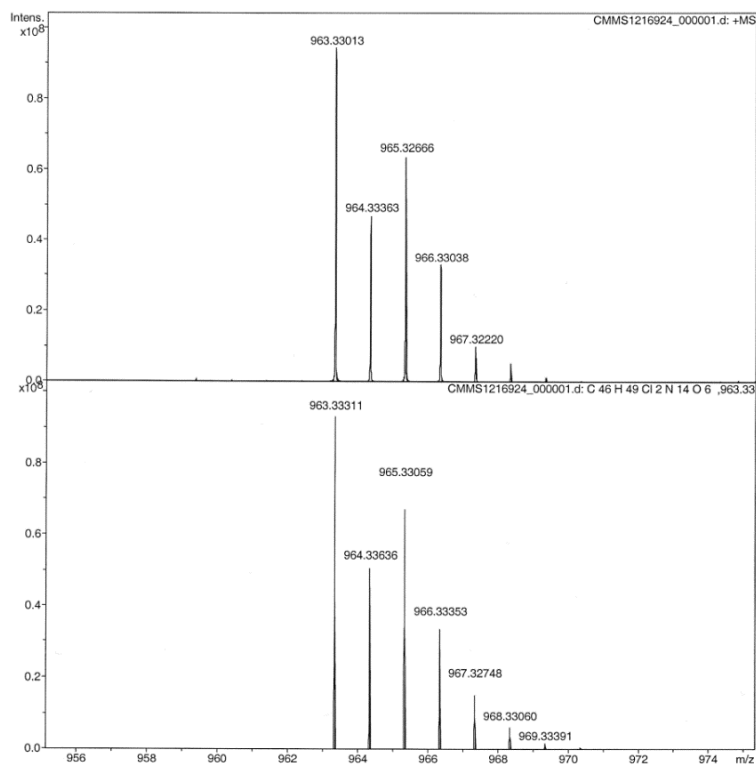


Figure S16. Isotopic distribution of  $[M+H]^+$  ion in the HRMS (ESI) spectrum of **1**.

## Infrared spectra

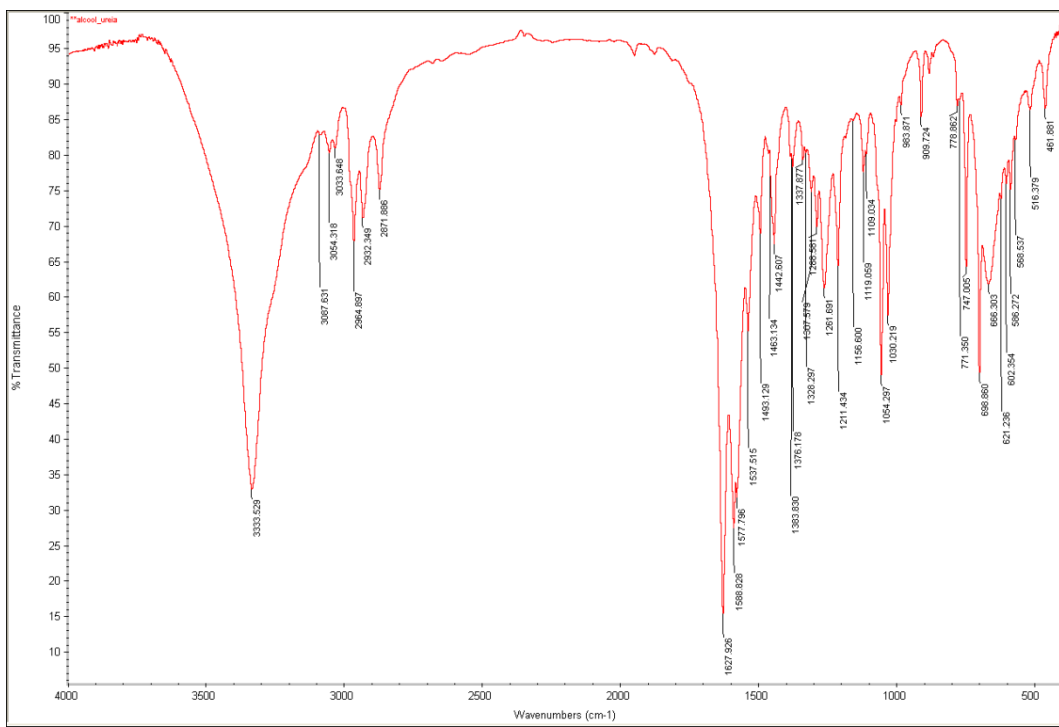


Figure S17. FTIR spectrum of **3** (KBr).

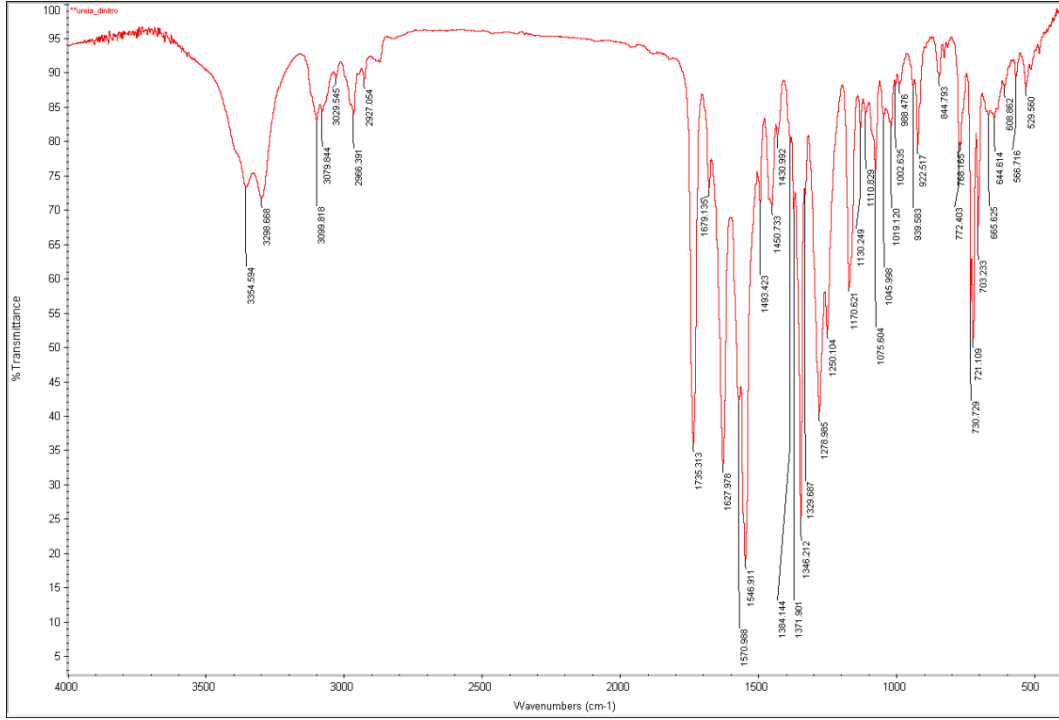


Figure S18. FTIR spectrum of **4** (KBr).

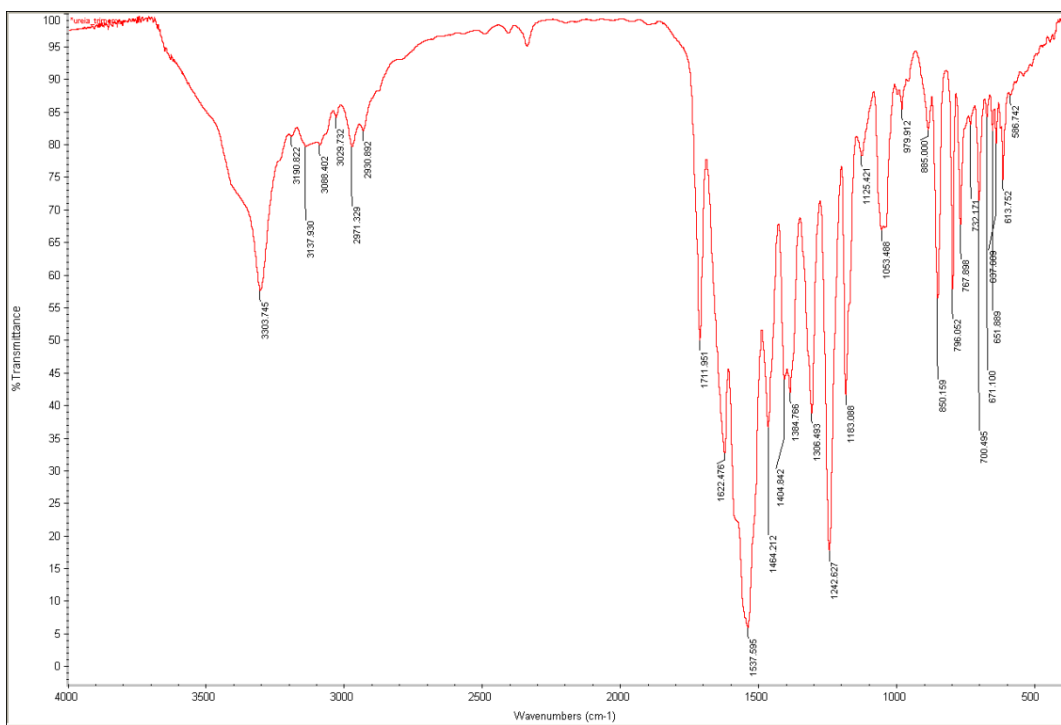


Figure S19. FTIR spectrum of **6** (KBr).

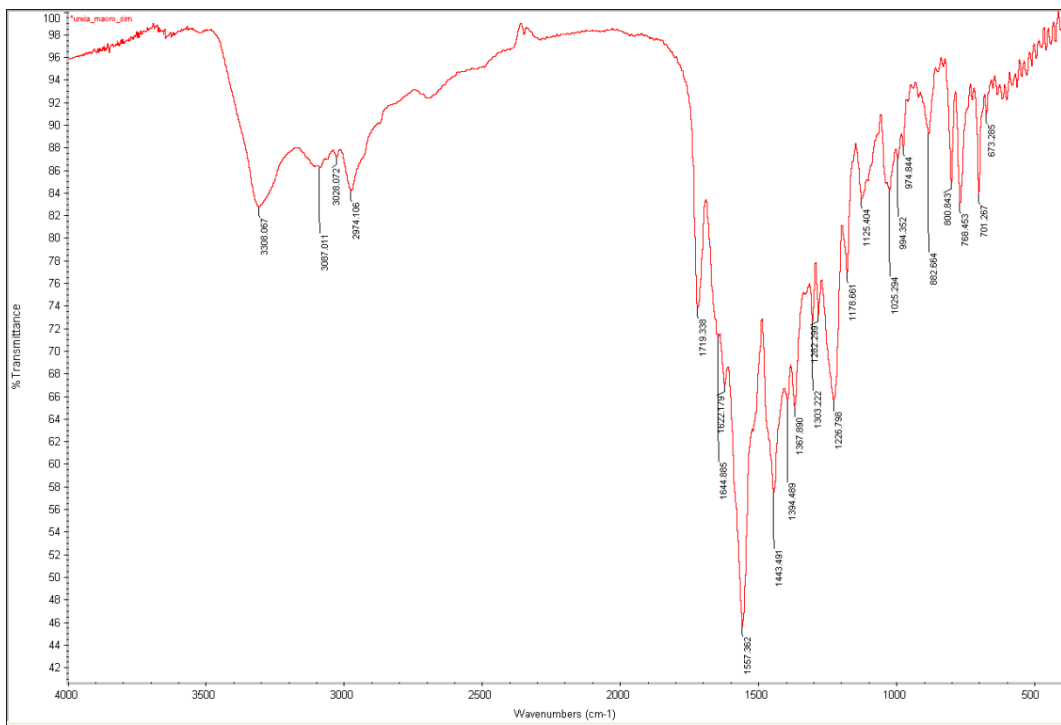


Figure S20. FTIR spectrum of **7** (KBr).

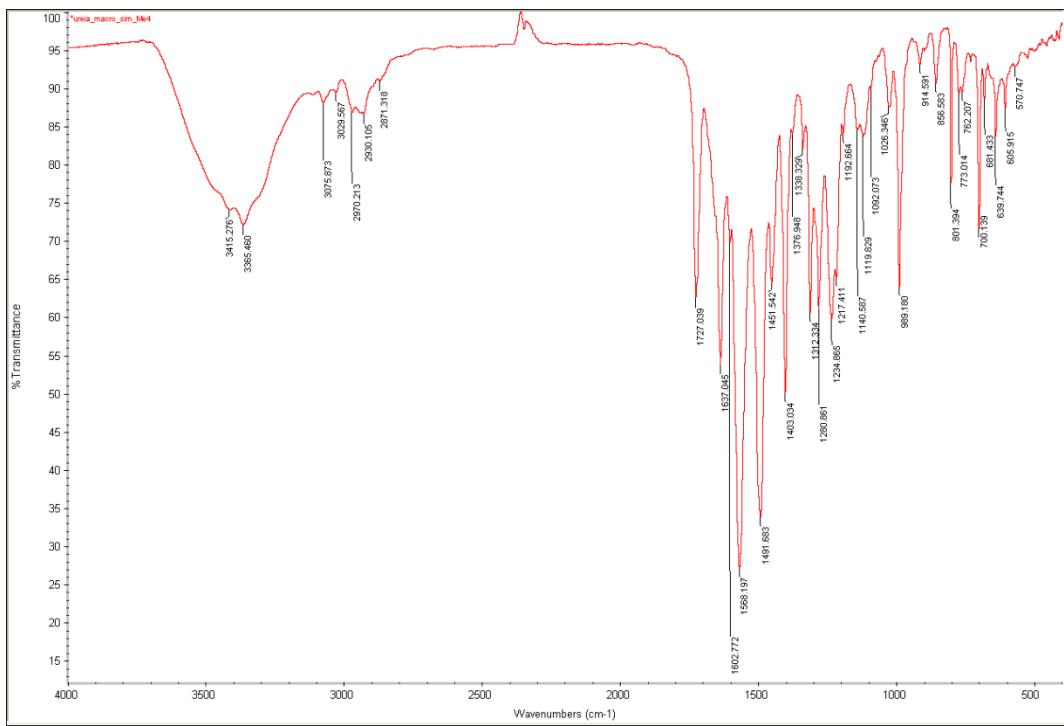


Figure S21. FTIR spectrum of 1 (KBr).

## VT $^1\text{H}$ NMR

- Tetrazacalix[2]arene[2]triazine **1** in  $\text{CDCl}_3$

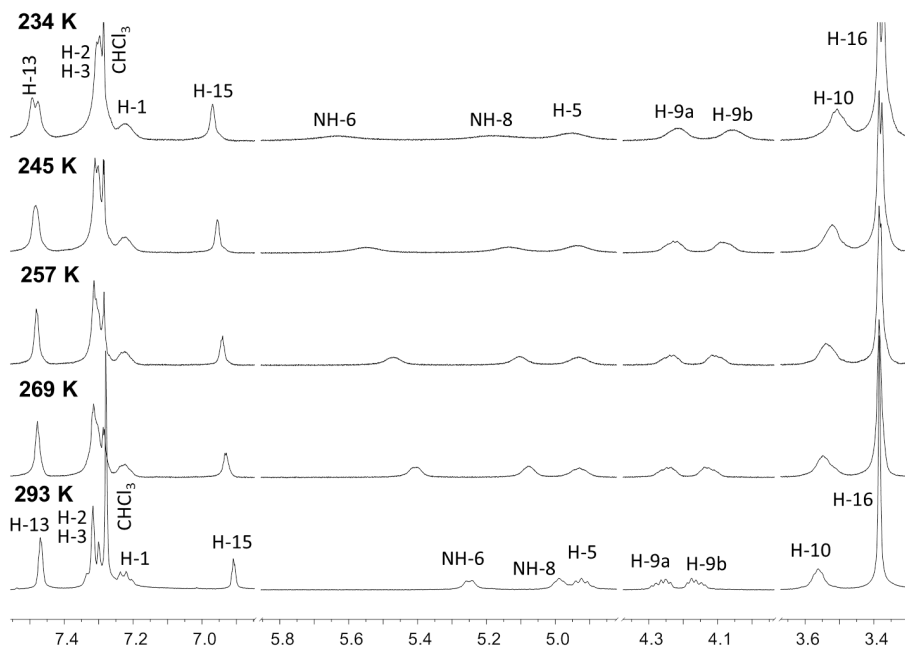


Figure S22.  $^1\text{H}$  NMR spectra of **1** at 293, 269, 257, 245 and 234 K in  $\text{CDCl}_3$ .

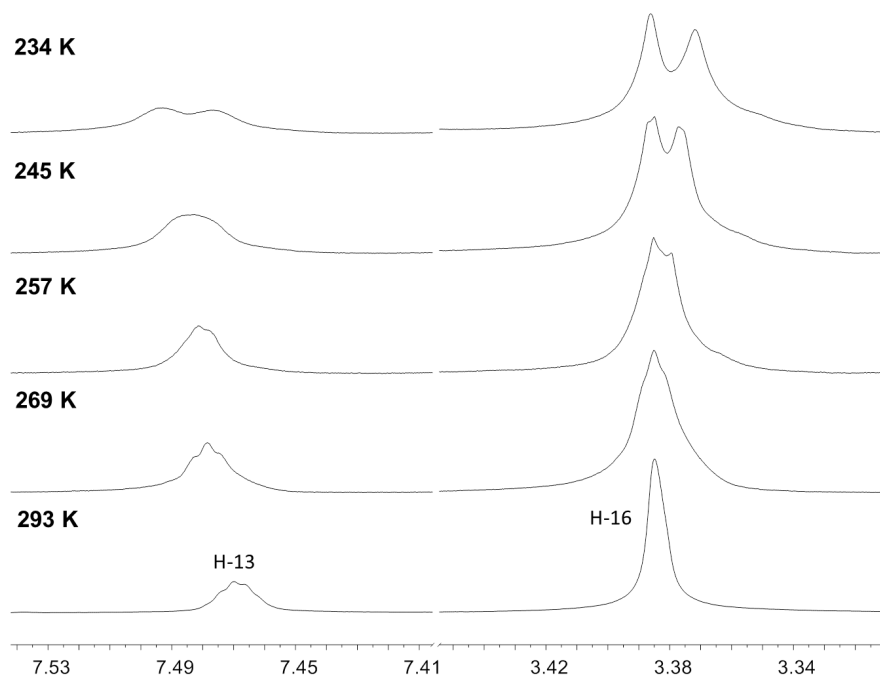


Figure S23. Close-up of H-13 and H-16 signals in the  $^1\text{H}$  NMR spectra of **1** at 293, 269, 257, 245 and 234 K in  $\text{CDCl}_3$ .

## X-ray Crystallography

Table S1. Dimensions of N-H $\cdots$ O hydrogen bonds of **1**.

Hydrogen Bonds [symmetry operation]	H $\cdots$ O ( $\text{\AA}$ )	N $\cdots$ O ( $\text{\AA}$ )	N-H $\cdots$ O ( $^{\circ}$ )
N(38D)-H $\cdots$ O(57D) [-1+x,y,z]	2.27	2.820(8)	121
N(38B)-H $\cdots$ O(57B) [x,-1+y,z]	2.23	2.844(8)	126
N(38A)-H $\cdots$ O(57A) [x,-1+y,z]	2.06	2.823(8)	144
N(38C)-H $\cdots$ O(40D) [x,1+y,z]	2.13	2.913(8)	148
N(41C)-H $\cdots$ O(40D) [x,1+y,z]	2.20	2.964(8)	145
N(55D)-H $\cdots$ O(57C) [1+x,y,z]	2.08	2.872(7)	148
N(55B)-H $\cdots$ O(40A) [1+x,1+y,z]	2.05	2.840(7)	149
N(55A)-H $\cdots$ O(40B)	2.10	2.900(7)	151
N(55C)-H $\cdots$ O(40C) [-1+x,y,z]	2.01	2.820(7)	152
N(58D)-H $\cdots$ O(57C) [1+x,y,z]	2.17	2.951(8)	147
N(58B)-H $\cdots$ O(40A) [1+x,1+y,z]	2.42	3.156(7)	141
N(58A)-H $\cdots$ O(40B)	2.22	3.003(7)	148

<sup>a)</sup> The atomic notation scheme used for the urea binding units is given in Figure S24, below.

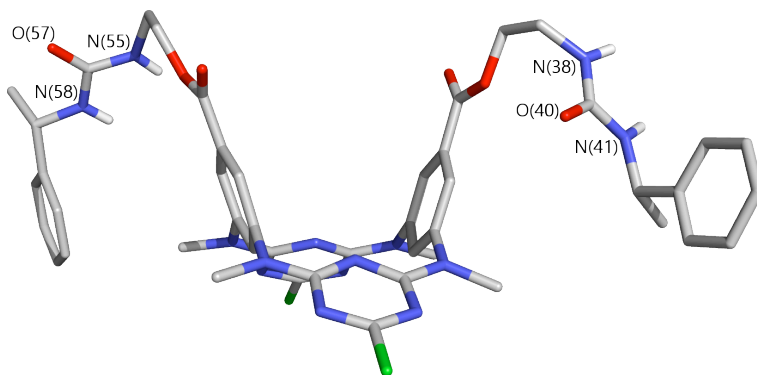


Figure S24. Atomic notation scheme of for the urea binding units of the four independent molecules (A-D) of **1**.

Table S2. Crystal data and structure refinement details for (NMe)4-azacalix[2]arene[2]triazine **1**.

Empirical formula	C <sub>46</sub> H <sub>48</sub> Cl <sub>2</sub> N <sub>14</sub> O <sub>6</sub>
Formula weight	963.88
Temperature/K	150(2)
Crystal system	Triclinic
Space group	P1
<i>a</i> /Å	14.9779(6)
<i>b</i> /Å	15.1104(6)
<i>c</i> /Å	23.1992(8)
$\alpha^{\circ}$	86.107(2)
$\beta^{\circ}$	81.276(2)
$\gamma^{\circ}$	67.781(2)
<i>V</i> /Å <sup>3</sup>	4804.1(3)
<i>Z</i>	4
$\rho_{\text{calc}}$ mg/mm <sup>3</sup>	1.333
$\mu$ /mm <sup>-1</sup>	0.199
<i>F</i> (000)	2016
Crystal size/mm <sup>3</sup>	0.280 × 0.060 × 0.030
Radiation	Mo-Kα ( $\lambda = 0.71073$ )
2 θ range for data collection	4.928 to 51.66
Index ranges	-18 ≤ <i>h</i> ≤ 18, -18 ≤ <i>k</i> ≤ 16, -28 ≤ <i>l</i> ≤ 28
Reflections collected	55221
Independent reflections	28172 [ $R_{\text{int}} = 0.0375$ , $R_{\text{sigma}} = 0.0654$ ]
Data/restraints/parameters	28172/3/2473
Goodness-of-fit on <i>F</i> <sup>2</sup>	1.037
Flack parameter	0.05(3)
Final <i>R</i> indexes [ <i>I</i> ≥ 2σ ( <i>I</i> )]	$R_I = 0.0606$ , $wR_2 = 0.1366$
Final R indexes [all data]	$R_I = 0.0886$ , $wR_2 = 0.1506$
Largest diff. peak/hole /eÅ <sup>-3</sup>	0.96/-0.36

## NMR titrations

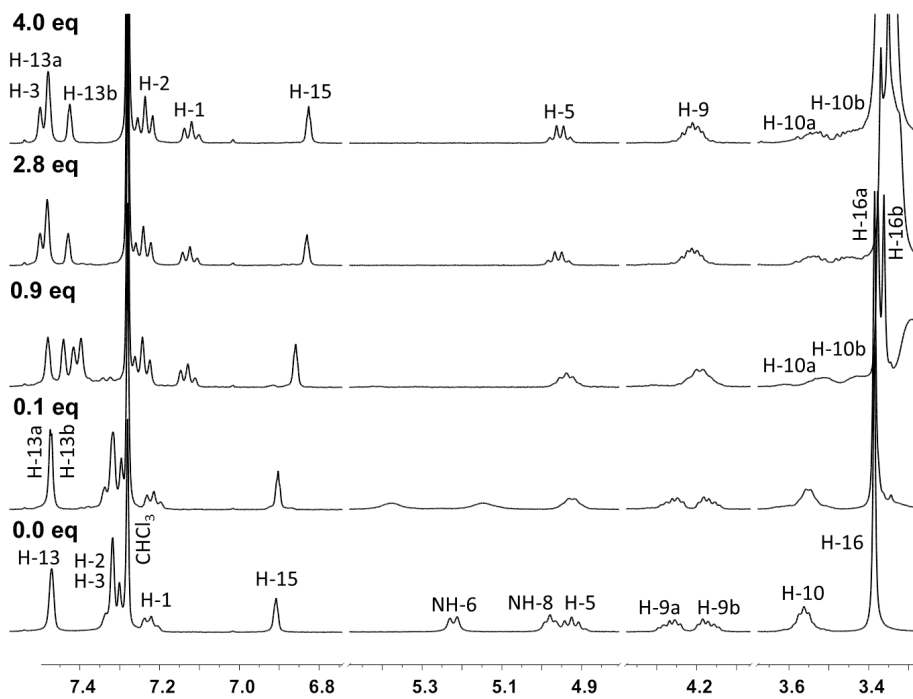


Figure S25. Relevant sections of  $^1\text{H}$  NMR spectra in  $\text{CDCl}_3$  of free **1** and upon addition of 0.1, 0.9, 2.8 and 4.0 equivalents of  $\text{ox}^{2-}$ .

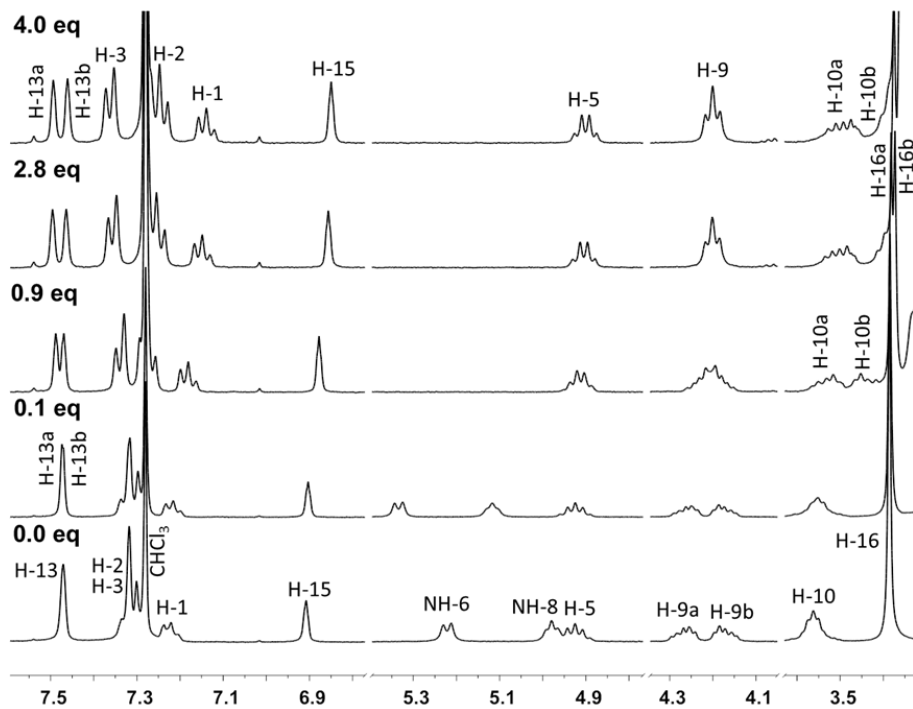


Figure S26. Relevant sections of  $^1\text{H}$  NMR spectra in  $\text{CDCl}_3$  of free **1** and upon addition of 0.1, 0.9, 2.8 and 4.0 equivalents of  $\text{mal}^{2-}$ .

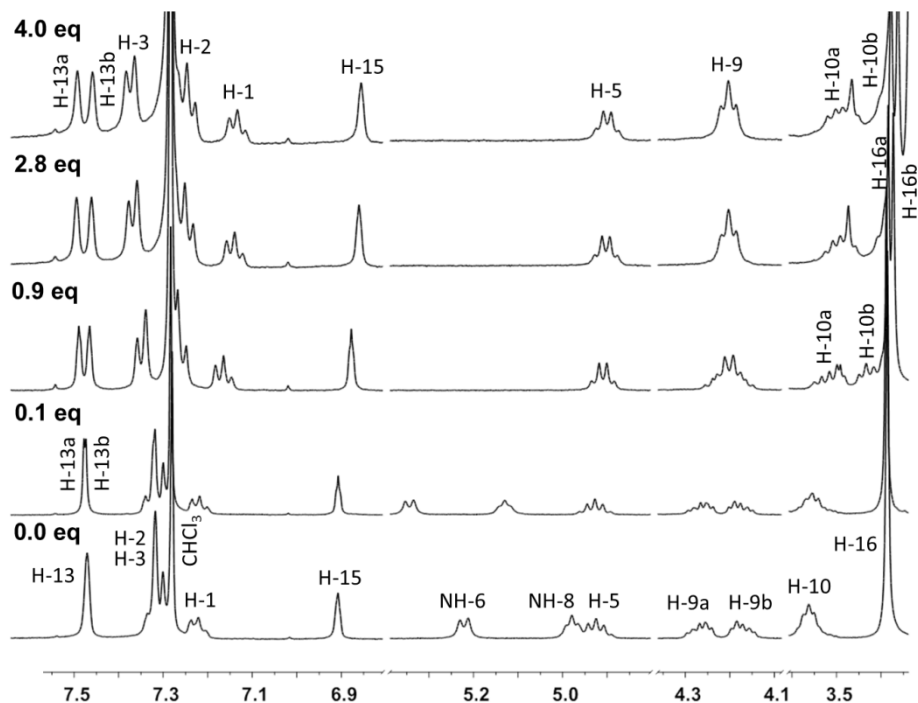


Figure S27. Relevant sections of  $^1\text{H}$  NMR spectra in  $\text{CDCl}_3$  of free **1** and upon addition of 0.1, 0.9, 2.8 and 4.0 equivalents of  $\text{su}c^{2-}$ .

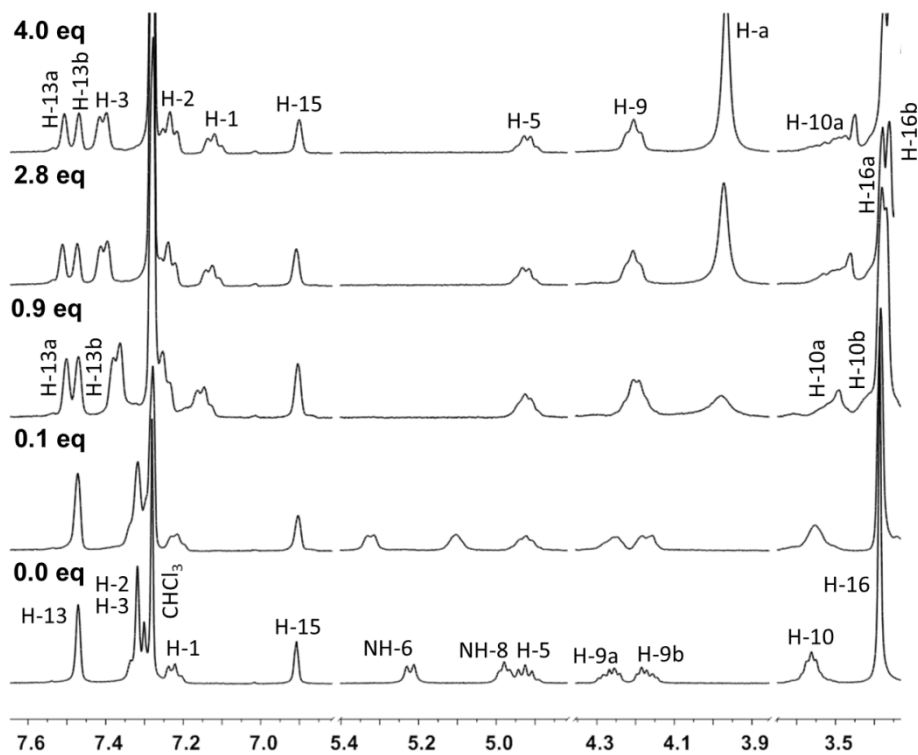


Figure S28. Relevant sections of  $^1\text{H}$  NMR spectra in  $\text{CDCl}_3$  of free **1** and upon addition of 0.1, 0.9, 2.8 and 4.0 equivalents of  $\text{dg}^{2-}$ .

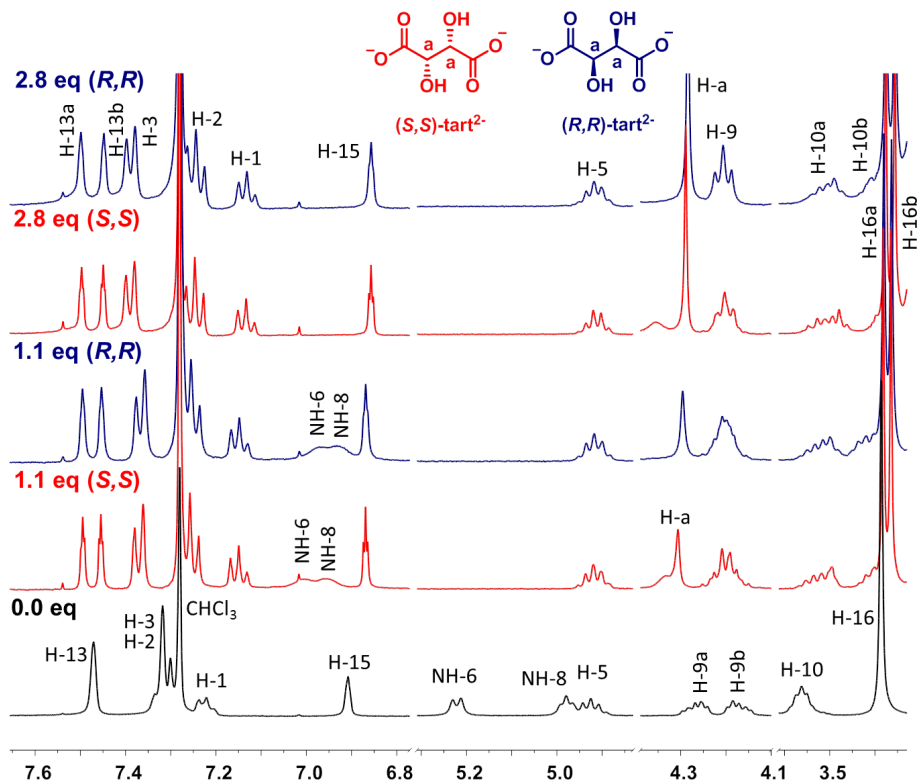


Figure S29. Relevant sections of  $^1\text{H}$  NMR spectra in  $\text{CDCl}_3$  of free **1** and upon addition of 1.1 and 2.8 equivalents of (*S,S*)- and (*R,R*)- $\text{tart}^{2-}$ .

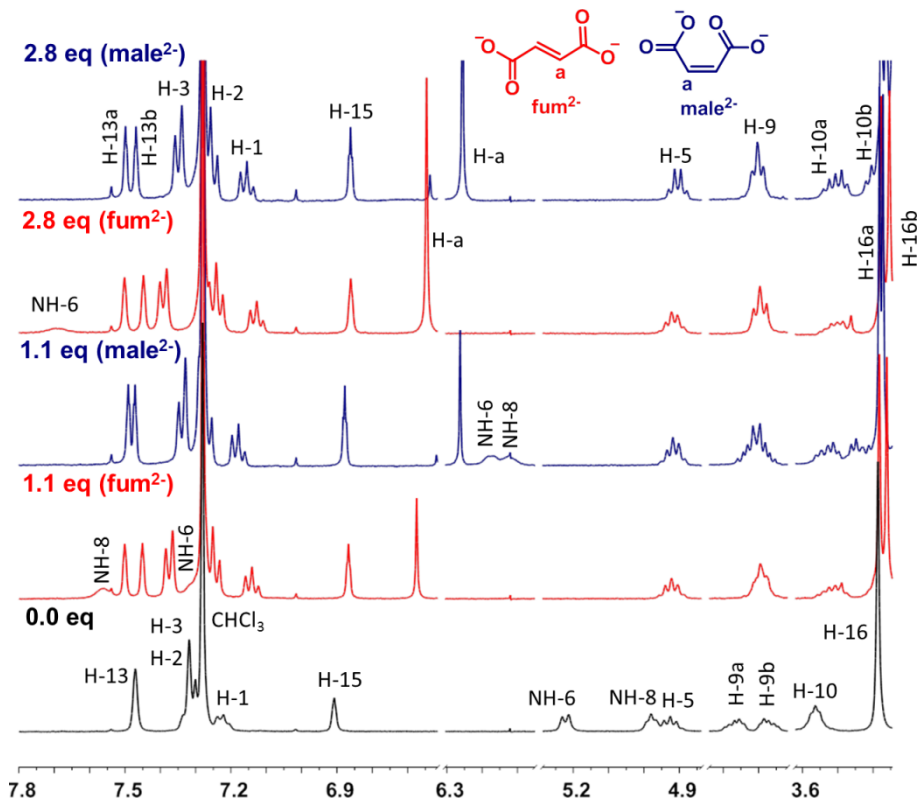


Figure S30. Relevant sections of  $^1\text{H}$  NMR spectra in  $\text{CDCl}_3$  of free **1** and upon addition of 1.1 and 2.8 equivalents of  $\text{fum}^{2-}$  and  $\text{male}^{2-}$ .

Table S3. Proton resonances used in the determination of  $K_{ass}$  for the associations between **1** and the dicarboxylate anion series  $\text{ox}^{2-}$ ,  $\text{mal}^{2-}$ ,  $\text{suc}^{2-}$ ,  $\text{glu}^{2-}$  and  $\text{dg}^{2-}$ .

Anions	$\text{ox}^{2-}$	$\text{mal}^{2-}$	$\text{suc}^{2-}$	$\text{glu}^{2-}$	$\text{dg}^{2-}$
Resonances	H-3	H-1	H-1	H-1	H-1
	NH-6	H-2	H-2	H-2	H-2
	NH-8	H-3	H-3	H-3	H-3
	H-15	H-5	H-5	H-10a	NH-6
		H-5'	H-5'		NH-8
		NH-6	NH-6		H-10a
		NH-8	NH-8		
		H-10a	H-10a		
		H-15	H-15		

Table S4. Proton resonances used in the determination of  $K_{ass}$  for the associations between **1** and the dicarboxylate anions  $(S,S)$ - ,  $(R,R)$ -tart $^{2-}$ , fum $^{2-}$  and male $^{2-}$ .

Anions	$(S,S)$ - , $(R,R)$ - tart $^{2-}$	fum $^{2-}$	male $^{2-}$
Resonances	H-1	H-1	H-1
	H-2	H-2	H-2
	H-3	H-3	H-3
	H-5'	H-5'	H-5'
	H-9a	NH-6	NH-6
	H-10a	NH-8	NH-8
	H-13b	H-13b	H-9a
	H-15	H-15	H-9b
	H-a	H-a	H-10a
			H-10b
			H-13b
			H-15
			H-a

## Job plots

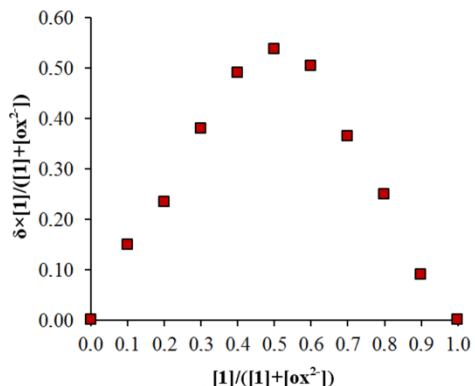


Figure S31. Job plot for  $\mathbf{1}\cdot\text{ox}^{2-}$  in  $\text{CDCl}_3$ .

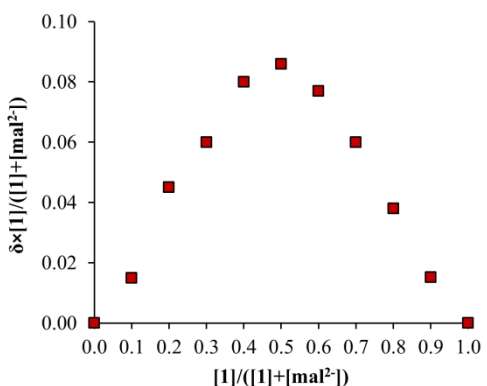


Figure S32. Job plot for  $\mathbf{1}\cdot\text{mal}^{2-}$  in  $\text{CDCl}_3$ .

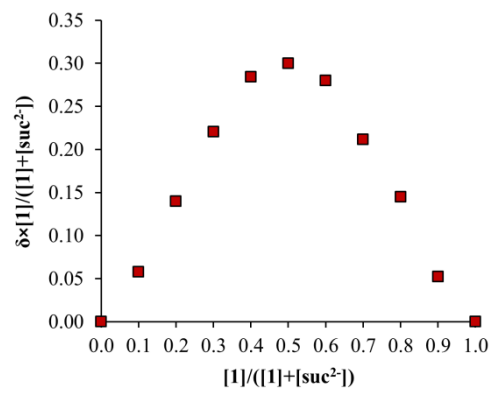


Figure S33. Job plot for  $\mathbf{1}\cdot\text{suc}^{2-}$  in  $\text{CDCl}_3$ .

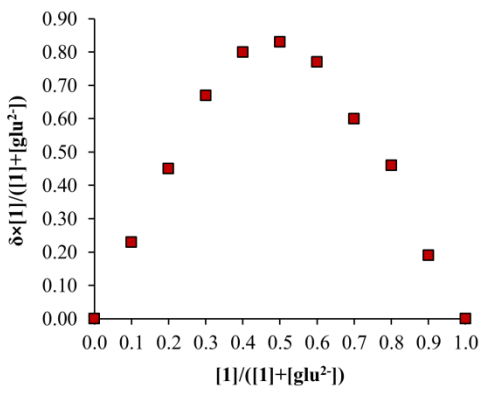


Figure S34. Job plot for  $\mathbf{1}\cdot\text{glu}^{2-}$  in  $\text{CDCl}_3$ .

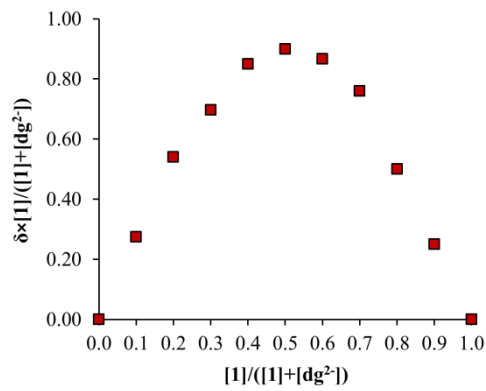


Figure S35. Job plot for  $\mathbf{1}\cdot\text{dg}^{2-}$  in  $\text{CDCl}_3$ .

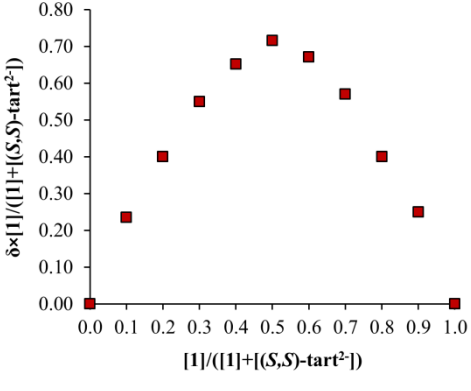


Figure S36. Job plot for  $\mathbf{1}\cdot(S,S)\text{-tart}^{2-}$  in  $\text{CDCl}_3$ .

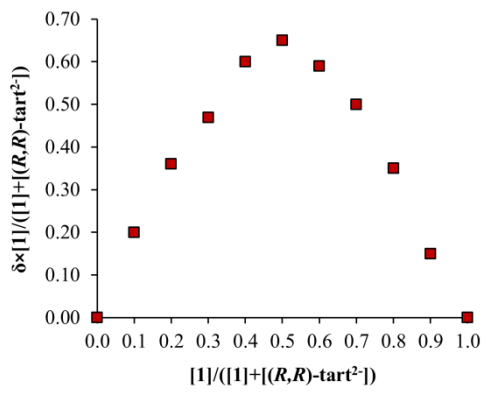


Figure S37. Job plot for  $\mathbf{1}\cdot(R,R)\text{-tart}^{2-}$  in  $\text{CDCl}_3$ .

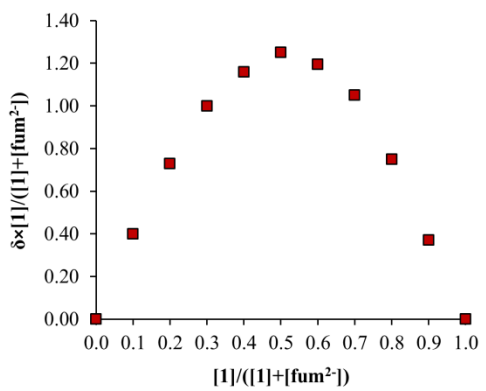


Figure S38. Job plot for  $\mathbf{1}\cdot\text{fum}^{2-}$  in  $\text{CDCl}_3$ .

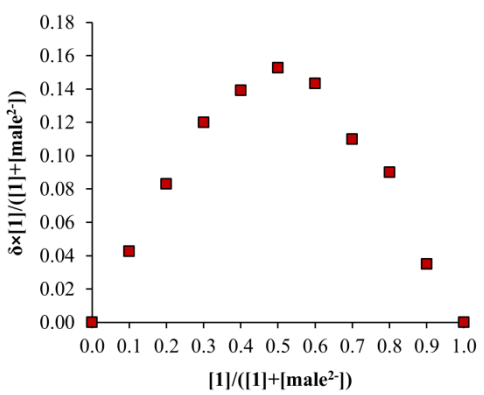


Figure S39. Job plot for  $\mathbf{1}\cdot\text{male}^{2-}$  in  $\text{CDCl}_3$ .

## Molecular dynamics

Table S5. Receptor's N<sub>urea</sub>⋯⋯N<sub>urea</sub> distances for the associations between **1** and ox<sup>2-</sup>, mal<sup>2-</sup>, suc<sup>2-</sup>, glu<sup>2-</sup>, dg<sup>2-</sup>, fum<sup>2-</sup> and male<sup>2-</sup>.

Anion association	Replicate	Average ± SD	Range [min ; max]
ox <sup>2-</sup>	R1 (50 ns)	7.703 ± 0.684	[5.260 ; 9.367]
	R2 (50 ns)	7.760 ± 0.596	[5.530 ; 9.747]
	R3 (50 ns)	7.755 ± 0.724	[5.279 ; 10.034]
	<i>All replicates (150 ns)</i>	7.739 ± 0.671	[5.260 ; 10.034]
mal <sup>2-</sup>	R1 (50 ns)	8.499 ± 0.662	[5.690 ; 10.445]
	R2 (50 ns)	8.756 ± 0.648	[5.908 ; 10.793]
	R3 (50 ns)	7.771 ± 0.818	[5.163 ; 10.614]
	<i>All replicates (150 ns)</i>	8.342 ± 0.826	[5.163 ; 10.793]
suc <sup>2-</sup>	R1 (50 ns)	9.033 ± 0.711	[5.771 ; 11.261]
	R2 (50 ns)	9.252 ± 0.720	[5.972 ; 11.403]
	R3 (50 ns)	9.454 ± 0.541	[6.405 ; 11.666]
	<i>All replicates (150 ns)</i>	9.246 ± 0.685	[5.771 ; 11.666]
glu <sup>2-</sup>	R1 (50 ns)	9.805 ± 1.109	[6.165 ; 12.421]
	R2 (50 ns)	10.344 ± 0.679	[6.586 ; 12.351]
	R3 (50 ns)	10.286 ± 0.775	[6.039 ; 13.032]
	<i>All replicates (150 ns)</i>	10.145 ± 0.907	[6.039 ; 13.032]
dg <sup>2-</sup>	R1 (50 ns)	10.294 ± 1.087	[6.307 ; 12.405]
	R2 (50 ns)	11.391 ± 0.335	[9.406 ; 12.615]
	R3 (50 ns)	10.542 ± 0.609	[6.249 ; 12.619]
	<i>All replicates (150 ns)</i>	10.743 ± 0.881	[6.249 ; 12.619]
fum <sup>2-</sup>	R1 (50 ns)	9.683 ± 0.690	[6.000 ; 12.233]
	R2 (50 ns)	9.468 ± 0.715	[6.357 ; 11.776]
	R3 (50 ns)	9.658 ± 0.518	[7.105 ; 11.395]
	<i>All replicates (150 ns)</i>	9.603 ± 0.654	[6.000 ; 12.233]
male <sup>2-</sup>	R1 (50 ns)	9.401 ± 0.529	[6.558 ; 11.368]
	R2 (50 ns)	5.254 ± 1.211	[2.874 ; 12.158]
	R3 (50 ns)	9.411 ± 0.494	[6.549 ; 11.211]
	R4 (50 ns)	7.228 ± 2.641	[2.868 ; 11.136]
	R5 (50 ns)	9.340 ± 1.306	[3.505 ; 11.313]
	R6 (50 ns)	9.437 ± 0.734	[5.346 ; 11.342]
	R7 (50 ns)	5.463 ± 2.119	[2.856 ; 15.866]
	<i>All replicates (350 ns)</i>	7.933 ± 2.332	[2.856 ; 15.866]

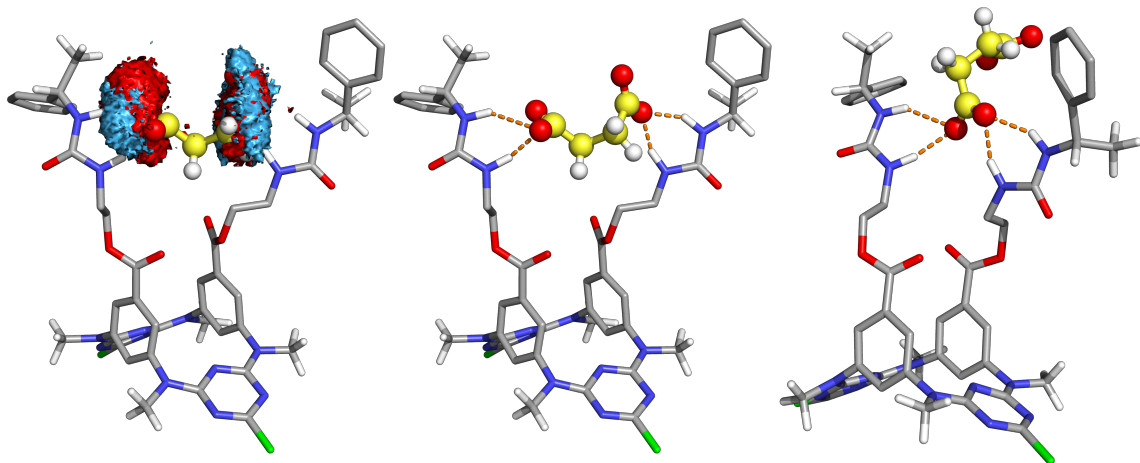


Figure S40. 3-D histogram for the third MD run of **1**· $\text{suc}^{2-}$  (left), and the respective type A (center) and type B (right) binding scenarios. Each carboxylate unit (shown either in red or blue) is represented by the positions occupied by its oxygen atoms, 5 or more times.

Table S6. Average  ${}^{\text{1}}\text{O}_2\text{C}\cdots\text{CO}_2^-$  distances collected for the associations between **1** and  $\text{ox}^{2-}$ ,  $\text{mal}^{2-}$ ,  $\text{suc}^{2-}$ ,  $\text{glu}^{2-}$ ,  $\text{dg}^{2-}$ ,  $\text{male}^{2-}$  and  $\text{fum}^{2-}$ .

Anion association	Average $\pm$ SD	Range [min ; max]
$\text{ox}^{2-}$	$2.907 \pm 0.049$	[2.694 ; 3.111]
$\text{mal}^{2-}$	$3.498 \pm 0.083$	[3.126 ; 3.865]
$\text{suc}^{2-}$	$4.692 \pm 0.419$	[3.424 ; 5.313]
$\text{glu}^{2-}$	$5.812 \pm 0.210$	[4.642 ; 6.376]
$\text{dg}^{2-}$	$5.908 \pm 0.253$	[4.186 ; 6.510]
$\text{fum}^{2-}$	$5.048 \pm 0.064$	[4.747 ; 5.333]
$\text{male}^{2-}$	$4.316 \pm 0.099$	[3.767 ; 4.776]

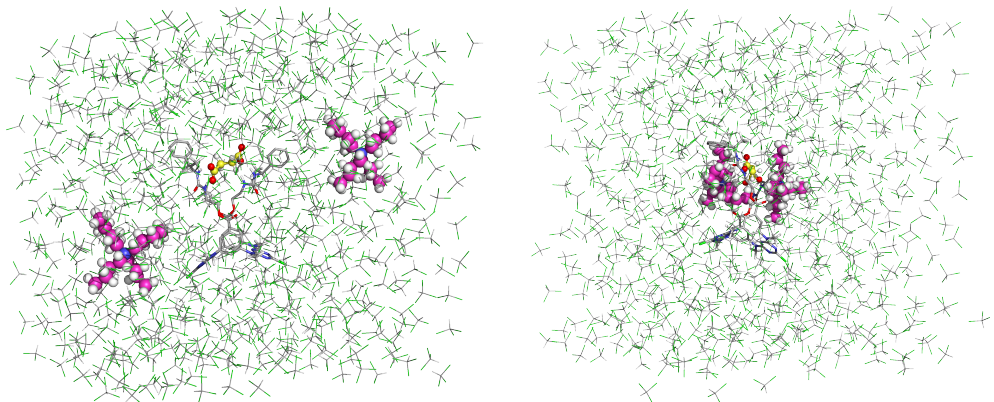


Figure S41. MD simulation cell of the system with the  $\text{suc}^{2-}$  anion complex, showing the position of the TBA counter-ions in the beginning (left) and at the end of the equilibration stage (right). The TBA molecules are shown in space-filling mode, with the carbon atoms in magenta, while the solvent molecules are shown in lines. Remaining details as given in Figure S40.

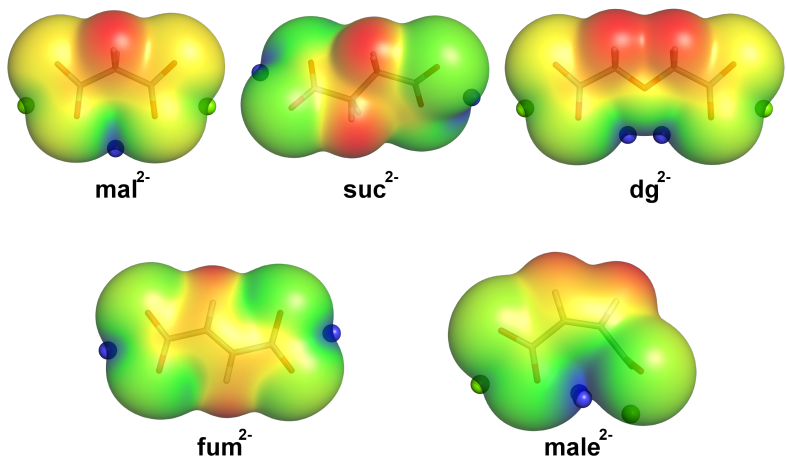


Figure S42. Electrostatic potential mapped on the molecular electron density surface (0.001 electrons per Bohr<sup>3</sup>) of mal<sup>2-</sup>, suc<sup>2-</sup>, dg<sup>2-</sup>, fum<sup>2-</sup> and male<sup>2-</sup>. The  $V_{S,\min}$  and  $V_{S,\text{carb}}$  are respectively represented by blue and green dots on the molecular surfaces. The colour scales range from blue to red as follows: mal<sup>2-</sup> [-242.8; -158.5 kcal mol<sup>-1</sup>]; suc<sup>2-</sup> [-207.7; -152.0 kcal mol<sup>-1</sup>]; dg<sup>2-</sup> [-222.4; -135.2 kcal mol<sup>-1</sup>]; fum<sup>2-</sup> [-206.7 ; -160.3 kcal mol<sup>-1</sup>]; and male<sup>2-</sup> [-229.8 ; -132.9 kcal mol<sup>-1</sup>].

Table S7. Additional force field parameters used to model the tetraazacalix[2]arene[2]triazine derivatives.

Bonds	$r_{\text{eq}}$ (Å)	$K_f$ (kcal mol <sup>-1</sup> Å <sup>-2</sup> )		
NH-CX	351.80	1.440		
NH-CT	462.60	1.355		
Angles	$\theta_{\text{eq}}$ (deg)	$K_f$ (kcal mol <sup>-1</sup> rad <sup>-2</sup> )		
nb-CT-NH	73.450	116.950		
NH-CX-ca	67.440	120.130		
hn-NH-CT	49.360	116.130		
hn-NH-CX	46.780	116.130		
CT-NH-CX	63.670	123.53		
CT-NH-c3	64.740	117.770		
CX-NH-c3	63.010	117.770		
CT-NH-ca	64.560	127.460		
CX-NH-ca	62.510	127.460		
Dihedral angles	IDIVF	$V_n$ (kcal mol <sup>-1</sup> )	$\gamma$ (deg)	$n$
X -CX-NH-X	4	14.5	180.0	2
X -CT-NH-X	2	9.6	180.0	2
van der Waals	$\epsilon$ (kcal mol <sup>-1</sup> )	$\sigma$ (Å)		
CT	1.9080	0.0860		
CX	1.9080	0.0860		
NH	1.8240	0.1700		

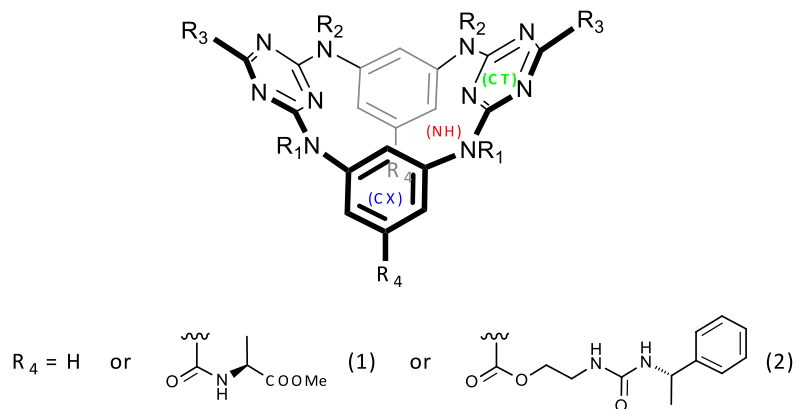


Figure S43. Sketch of tetraazacalix[2]arene[2]triazine derivatives showing the atom types' positions. The R<sub>1</sub>, R<sub>2</sub> and R<sub>3</sub> substituents are given in Table S8.

Table S8. RMSD values ( $\text{\AA}$ ) between the single crystal structures of tetraazacalix[2]arene[2]triazine derivatives and gas-phase structures obtained MM energy minimization with GAFF default parameters (GFD) and optimized parameters (OPT), respectively.

Macrocycle	Substituents			RMSDs <sup>a), b)</sup>				
	R <sub>1</sub>	R <sub>2</sub>	R <sub>3</sub>	R <sub>4</sub>	GFD	OPT		
<b>1<sup>c)</sup></b>	Me	Me	Cl	(2)	1.120	0.182	2.48	0.412
FAYZUB <sup>d)</sup>	H	H	Cl	H	0.990	0.895	0.493	0.372
FAZBAK <sup>d)</sup>	H	Me	Cl	H	0.264	0.258	0.225	0.231
FAZBIS <sup>d)</sup>	Me	Me	Cl	H	0.398	0.279	0.286	0.232
YESRIY <sup>d)</sup>	PMB <sup>e)</sup>	H	Cl	H	1.743	0.655	0.312	0.256
YESROE <sup>d)</sup>	H	Bn <sup>f)</sup>	Cl	H	0.786	0.542	0.434	0.174
YESREU <sup>d)</sup>	PMB <sup>e)</sup>	Bn <sup>f)</sup>	Cl	H	1.291	0.524	0.497	0.200
YESRUK <sup>d)</sup>	PMB <sup>e)</sup>	PMB <sup>e)</sup>	NMe <sub>2</sub>	H	1.538	0.568	1.242	0.236
YEASSAR <sup>d)</sup>	Bn <sup>f)</sup>	Bn <sup>f)</sup>	Cl	H	0.683	0.329	0.615	0.165
VUMNOH <sup>d)</sup>	H	H	OMe	H	0.584	0.535	0.203	0.203
NAQDEQ <sup>d)</sup>	H	H	Cl	(1)	1.818	0.649	0.572	0.218
<b>L2<sup>g)</sup></b>	Me	Me	Cl	(1)	1.168	0.253	1.418	0.430
BIVCUG <sup>d)</sup>	H	H	N(C <sub>6</sub> H <sub>13</sub> ) <sub>2</sub>	H	1.150	0.605	0.559	0.280
<b>L3<sup>g)</sup></b>	Me	Me	N(C <sub>6</sub> H <sub>13</sub> ) <sub>2</sub>	H	2.102	0.574	0.419	0.135
BIVCIU <sup>d)</sup>	CH <sub>2</sub> CO <sub>2</sub> Me	CH <sub>2</sub> CO <sub>2</sub> Me	Cl	H	0.759	0.294	0.636	0.163
BIVCOA <sup>d)</sup>	CH <sub>2</sub> CO <sub>2</sub> Me	CH <sub>2</sub> CO <sub>2</sub> Me	NMe <sub>2</sub>	H	1.642	0.584	0.525	0.300

<sup>a)</sup> All RMSD values calculated excluding the hydrogen atoms; <sup>b)</sup> Values in italic are for tetraazacalix[2]arene[2]triazine platform; <sup>c)</sup> This work; <sup>d)</sup> CSD REFCODES; <sup>e)</sup> p-methoxy-benzene; <sup>f)</sup> benzyl; <sup>g)</sup> unpublished results.